Chemical Science

ROYAL SOCIETY OF CHEMISTRY

EDGE ARTICLE

View Article Online
View Journal | View Issue

Cite this: *Chem. Sci.*, 2022, **13**, 7907

All publication charges for this article have been paid for by the Royal Society of Chemistry

Received 21st February 2022
Accepted 28th May 2022

DOI: 10.1039/d2sc01088g

rsc.li/chemical-science

Between imide, imidyl and nitrene – an imido iron complex in two oxidation states†

Sascha Reith, [a] Serhiy Demeshko,[b] Beatrice Battistella, [c] Alexander Reckziegel,[a] Christian Schneider, [a] Andreas Stoy,[a] Crispin Lichtenberg, [a] Franc Meyer, [b] Dominik Munz *[de] and C. Gunnar Werncke *[a]

Imidyl and nitrene metal species play an important role in the *N*-functionalisation of unreactive C–H bonds as well as the aziridination of olefines. We report on the synthesis of the trigonal imido iron complexes $[Fe(NMes)L_2]^{0,-}$ (L = –N{Dipp}SiMe$_3$); Dipp = 2,6-diisopropyl-phenyl; Mes = (2,4,6-trimethylphenyl) *via* reaction of mesityl azide (MesN$_3$) with the linear iron precursors $[FeL_2]^{0,-}$. UV-vis-, EPR-, ^{57}Fe Mössbauer spectroscopy, magnetometry, and computational methods suggest for the reduced form an electronic structure as a ferromagnetically coupled iron(II) imidyl radical, whereas oxidation leads to mixed iron(III) imidyl and electrophilic iron(II) nitrene character. Reactivity studies show that both complexes are capable of H atom abstraction from C–H bonds. Further, the reduced form $[Fe(NMes)L_2]^-$ reacts nucleophilically with CS_2 by inserting into the imido iron bond, as well as electrophilically with CO under nitrene transfer. The neutral $[Fe(NMes)L_2]$ complex shows enhanced electrophilic behavior as evidenced by nitrene transfer to a phosphine, yet in combination with an overall reduced reactivity.

Introduction

Imido complexes of the late 3d-transition metals play a crucial role in nitrene transfer catalysis.[1,2] As such there is an innate interest in understanding the structural and electronic features of the central imido metal unit to control and predict its reactivity.[3–5] The imido ligand is classically regarded as a dianionic imide $[NR]^{2-}$ that forms either a double or triple bond, as it is the case for early transition metals.[2,6] For the 3d-metals, the metal–imido bond becomes more covalent and p → d donation is reduced due to (partially) filled d-orbitals. This may result in intriguing bonding situations, namely metal stabilized imidyl radical $[NR]^{\bullet-}$ or even electrophilic nitrene $[NR]^0$ ligands, that are highly reactive.[4,5] The former was observed in a few instances for iron,[7,8] cobalt[9,10] and nickel.[11,12] 3d-Metal nitrenes are mostly known for copper,[13–15] with only two isolated examples.[13,15] Given the overall reactive nature of late 3d-metal imido species, the impact of oxidation state changes onto the imido unit is only partially understood. For low-spin complexes, mostly found for isolable and rather unreactive late 3d-metal imidos, few reports of one-electron oxidation showed contraction of the imido metal bond.[12,16–20] This can be explained by a metal centred oxidation, accompanied with ion radius contraction as well as increased p → d donation and depopulation of *anti*-bonding molecular orbitals.[5,21] Contrastingly, in the only two reports of oxidation of high-valent high-spin 3d-metal imidos M–N bond elongation took place (Fig. 1).[9,22]

This was attributed to a ligand-centred oxidation and spin density increase at the imido ligand, that resulted in an imidyl radical character. For a pseudo-trigonal bipyramidal imido

[a]*Philipps-University Marburg, Department of Chemistry, Hans-Meerwein-Str. 4, D-35037 Marburg, Germany. E-mail: gunnar.werncke@chemie.uni-marburg.de*
[b]*University of Göttingen, Institute of Inorganic Chemistry, Tammannstr. 4, D-37077 Göttingen, Germany*
[c]*Humboldt-University, Berlin Institute for Chemistry, Brook-Taylor-Str. 2, D-12489 Berlin, Germany*
[d]*Saarland University, Inorganic Chemistry: Coordination Chemistry, Campus C4.1, D-66123 Saarbrücken, Germany. E-mail: dominik.munz@uni-saarland.de*
[e]*Friedrich-Alexander University Erlangen-Nürnberg, Inorganic Chemistry, Egerlandstr. 1, D-91058 Erlangen, Germany*

† Electronic supplementary information (ESI) available: General, experimental, analytical (NMR, IR, UV/vis, ^{57}Fe Mössbauer and EPR spectroscopy, SQUID magnetometry, cyclovoltammetry), computational and crystallographic details. CCDC 2130485–2130488. For ESI and crystallographic data in CIF or other electronic format see **https://doi.org/10.1039/d2sc01088g**

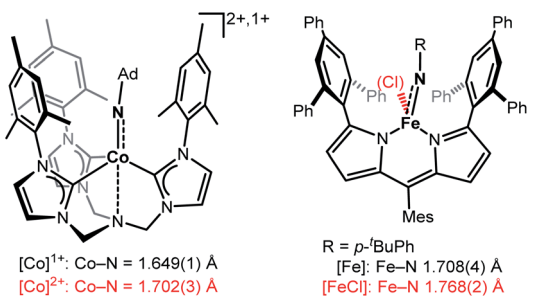

Fig. 1 Examples of imido metal complex oxidation leading to M–N bond lengthening and imidyl character (Ad = adamantyl, Mes = 2,4,6-trimethylphenyl).[7–9]

cobalt complex (Fig. 1, left) oxidation led to a switch from the high-spin to the low-spin configuration (d^5, $S = 1/2$).[9] For a trigonal planar dipyrromethane (dpm) based imido iron complex (Fig. 1, right) the high-spin state persisted, with an increase of the coordination number.[22]

Building on recent examples of low-coordinate imido cobalt silylamides in higher spin-states[23,24] we report herein the trigonal iron imido complexes $[Fe(NMes)L_2]^{0,-}$ (L = –N(Dipp)$SiMe_3$; Dipp = 2,6-diisopropyl-phenyl; Mes = 2,4,6-trimethyl-phenyl) in the formal oxidation states +III and +IV, which can be interconverted by oxidation/reduction. Detailed spectroscopic and computational analyses reveal the ambiguous electronic structure of both complexes. The anionic $[Fe(NMes)L_2]^-$ is described best as an iron(II) imidyl complex whereas the oxidized neutral $[Fe(NMes)L_2]^0$ shares iron(III) imidyl and iron(II) nitrene character. The electronic ambiguity is reflected best by $[Fe(NMes)L_2]^-$ which shows ambiphilic, *i.e.* combined nucleophilic and electrophilic behaviour, whereas the nucleophilicity is lost upon oxidation to $[Fe(NMes)L_2]^0$.

Results and discussion

The imido iron complex K{m}[Fe(NMes)L_2], K{m}[**1**] (*m* = crypt.222), was obtained as a green crystalline solid (yield 86%) by treatment of a solution of the linear iron(I) precursor K{m}[FeL_2] in a mixture of thf/Et_2O (1 : 3) with $MesN_3$ at −40 °C (Scheme 1). X-ray diffraction analysis revealed for the complex anion $[\mathbf{1}]^-$ (Fig. 2) a Fe–N_{imido} bond length of 1.7744(15) Å and a Fe–N–C_{Aryl} bond angle of 173.6(13)°. Usually, imido–iron bond lengths of low-spin complexes range from 1.65 to 1.70 Å.[16–18,25,26] Longer Fe–N_{imido} bonds are rarely observed, but are found for high-spin iron imidos with[7,8,27] or without[28] imidyl character on the nitrogen atom as well as an anionic iron(II) imide.[20] $[\mathbf{1}]^-$ shows a short N–C_{Aryl} bond of 1.339(2) Å, which is in line with aforementioned high-spin imido iron complexes with C–N double bond character. The observed structural metrics closely resemble the related high-spin imidyl cobalt(II) complex $[Co(NDipp)L_2]^-$ (*e.g.* M–N_{imide} 1.751(2) Å, N–C_{Aryl} 1.347(2) Å),[23] which suggested for $[\mathbf{1}]^-$ also an iron(II) imidyl-like bonding situation on a structural level.

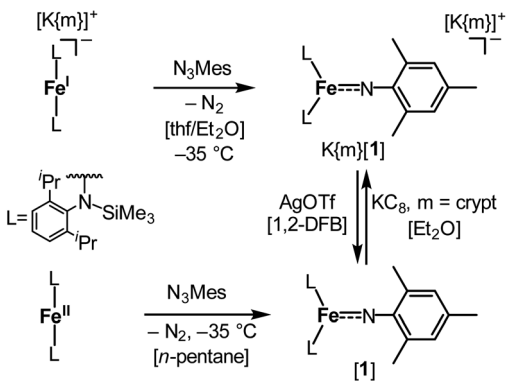

Scheme 1 Synthesis of complexes K{m}[Fe(NMes)L_2], K{m}[**1**] (*m* = crypt.222), and [Fe(NMes)L_2], [**1**], as well as their interconversion by oxidation and reduction.

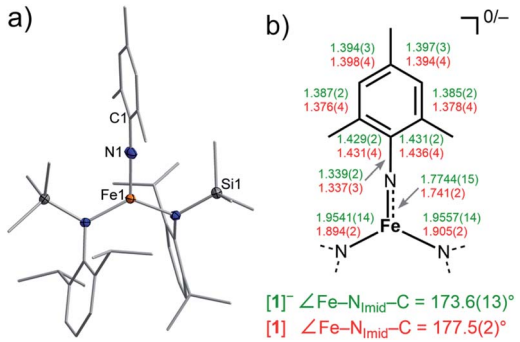

Fig. 2 (a) Solid state structure of [**1**]. The H atoms are omitted for clarity. (b) Selected bond metrics for $[\mathbf{1}]^-$ (green) and [**1**] (red) [Å].

Given the scarcity of unambiguously identified iron bound imidyl units, namely only tetrahedral iron(III) imidyls of the type [(dpm)Fe(Cl)(NR)] from Betley and co-workers (Fig. 1, right),[7,8,22] we sought further insights into the electronic situation of $[\mathbf{1}]^-$. Magnetic measurements (SQUID) on solid material yielded an $\chi_M T$ value of 4.4 $cm^3\ mol^{-1}$ K (corresponding to an effective magnetic moment of $\mu_{eff} = 5.93\ \mu_B$) at 210 K (Fig. 3a).

This is close to the spin-only value of a sextet state ($\mu_{s.o.} = 5.92\ \mu_B$) and can be rationalized either by an iron(II) ion ferromagnetically coupled to an imidyl radical anion, or by a high-spin iron(III) imide. Upon cooling, a sharp drop is observed below 20 K, which is attributed to zero-field splitting (simulation of the $\chi_M T$ data gave $g = 2.01$, $D = 2.5\ cm^{-1}$; see ESI† for more details).

To assess the oxidation state of the metal in $[\mathbf{1}]^-$, zero-field ^{57}Fe Mössbauer spectroscopy was employed. It revealed a doublet with an isomer shift (IS) of $\delta = 0.43$ mm s^{-1} (at 80 K) and a large quadrupole splitting (QS) of $|\Delta E_Q| = 4.18$ mm s^{-1} (Fig. 3b). The IS is similar to that of the related three-coordinate high-spin iron(III) imide ([(dpm)Fe(N{*p*-^{t}Bu-Ph})]: $\delta = 0.44$ mm s^{-1}, $|\Delta E_Q| = 0.00$ mm s^{-1}, at 200 K; Fig. 1, right),[8,27,28] but also to that of the anionic iron(II) imide [($Ph_2B\{^tBuIM\}_2$)Fe(NDipp)]$^-$ ($\delta = 0.46$ mm s^{-1}, $|\Delta E_Q| = 1.45$ mm s^{-1}, at 80 K).[20] The IS of K{m}[**1**] ranges between those of the diferric and diferrous silylamide complexes $[(L_2Fe)_2(\mu\text{-}S)]^{2-,0}$ at 80 K with unambiguous trigonal iron(II) ($\delta = 0.59$ mm s^{-1}) and iron(III) ions ($\delta = 0.29$ mm s^{-1}).[29] The large QS of K{m}[**1**] is remarkable and would generally point to divalent iron. However, also for a number of planar iron(III) complexes large QS have been reported.[30] Moreover, related (pseudo-)trigonal iron silylamides exhibit substantially larger QS in the ferric compared to the ferrous state (*e.g.* $[(L_2Fe)_2(\mu\text{-}S)]^{2-,0}$: $|\Delta E_Q| = 0.22$ mm s^{-1} (Fe^{2+}), 3.70 mm s^{-1} (Fe^{3+}), at 80 K;[29] $[Fe(N(SiMe_3)_2)_3]^{-,0}$: $|\Delta E_Q|$ (Fe^{2+}) = 0.60 mm s^{-1} at 3 K,[31] $|\Delta E_Q|$ (Fe^{3+}) 5.12 mm s^{-1} at 77 K [32]).

X-band EPR spectroscopic examination of $[\mathbf{1}]^-$ at 13 K yielded an axial signal with $g_1 = 6.5$, $g_2 = 4.28$, $g_3 = 4.18$ (A_1 (^{14}N) = 107 G, A_2 (^{14}N) = 1.7 G, A_3 (^{14}N) = 20.5 G; see ESI†), the large ^{14}N hyperfine coupling implicating substantial spin density on nitrogen. This is consistent with substantial imidyl character in $[\mathbf{1}]^-$, and also aligns with its structural features.

Next, we wanted to elaborate if we could electrochemically attenuate the electronic situation of $[\mathbf{1}]^-$. Cyclic voltammetry

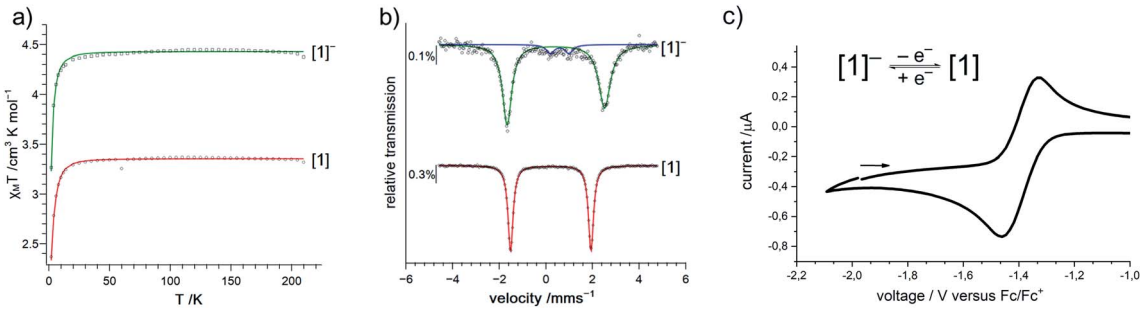

Fig. 3 (a) Variable-temperature magnetic susceptibility of solid K{m}[**1**] (green) and [**1**] (red) in the range of 2–210 K. (b) Zero-field ^{57}Fe Mössbauer spectra of solid K{m}[**1**] (green) and [**1**] (red) at 80 K. Parameters for K{m}[**1**]: $\delta = 0.43$ mm s^{-1}, $|\Delta E_Q| = 4.18$ mm s^{-1} (92%); [**1**]: $\delta = 0.21$ mm s^{-1}, $|\Delta E_Q| = 3.45$ mm s^{-1}. (c) Cyclic voltammogram of K{m}[**1**] (500 mV s^{-1}, thf, 0.1 m nBu$_4$ [PF$_6$] *vs.* Fc/Fc$^+$).

examination showed a reversible redox event at $E_{1/2} = -1.4$ V at 500 mV s^{-1} (THF, *vs.* Fc/Fc$^+$, Fig. 3c), that becomes irreversible upon lowering the scan rate to 50 mV (Fig. S24†). The potential is in line with those for the oxidation of imido iron(III) and imido iron(II) species (≈ -1.3 to -0.7 V).[16,17,33] Gratifyingly, chemical oxidation of [**1**]$^-$ in 1,2-difluorobenzene with AgOTf (OTf$^-$ = F$_3$CSO$_3^-$) led to the formation of a new paramagnetic species which we attributed to neutral [**1**]. [**1**] could not be isolated *via* this pathway due to partial degradation, but was independently synthesized by reacting [FeL$_2$] with MesN$_3$ in *n*-pentane (yield 64%, Scheme 1). It can be reduced back to [**1**]$^-$ by KC$_8$ in the presence of crypt.222, evidencing the possibility of their chemical interconversion. X-ray diffraction analysis of [**1**] showed in comparison with [**1**]$^-$ that all metal–nitrogen bonds contract upon oxidation with otherwise little changes in the Fe–N–C unit (Fe–N$_{imide}$ 1.741(2) Å, Fe–N$_{imide}$–C$_{Aryl}$ 177.5(2)°, N$_{imide}$–C$_{Aryl}$ 1.337(3) Å; Fig. 2, right), where the contraction of the Fe–N amide bonds was slightly more pronounced. Thus, it was suggestive of at least partial metal based oxidation. This was corroborated by ^{57}Fe Mössbauer spectroscopy showing an IS of $\delta = 0.21$ mm s^{-1} for [**1**] (*vs.* [**1**]$^-$: 0.43 mm s^{-1}). It is in line with shorter Fe–ligand bonds and by that with the decrease of the radial extension of the 4 s wave function in case of the oxidized species [**1**]. Further, a negative correlation of the IS with the Fe oxidation state is usually valid for high spin complexes.[34] The QS for [**1**] is with $|\Delta E_Q| = 3.56$ mm s^{-1} (*vs.* [**1**]$^-$: 4.18 mm s^{-1}) only slightly reduced, and indicates a similar electron density distribution (electric field gradient) in both complexes. The IS value of [**1**] is distinct from those of iron(IV) imides, which are found between -0.09 and -0.52 mm s^{-1}.[26,35] This precludes for [**1**] a formulation as an iron(IV) imide. Accordingly, its IS value is closer to those of high-spin iron(III) imides ($\delta = 0.37$–0.47 mm s^{-1}, $|\Delta E_Q| \approx 0$ mm s^{-1} at 200 K),[8,27,28] a trigonal intermediate-spin iron(III) imide ($\delta = 0.25$ mm s^{-1}, $|\Delta E_Q| = 1.32$ mm s^{-1}, at 200 K)[20] or four-coordinate high-spin iron(III) imidyls (*e.g.* [(dpm)Fe(N{*p*-^{t}Bu-C$_6$H$_4$})Cl] $\delta = 0.28$ mm s^{-1}, $|\Delta E_Q| = 2.22$ mm s^{-1}, at 90 K).[7,8,22] Solid state SQUID measurements on [**1**] (Fig. 3a) gave a $\chi_M T$ value of 3.3 cm^3 mol^{-1} K ($\mu_{eff} = 5.14\ \mu_B$) at 210 K with $D = -3.5$ cm^{-1} and $g = 2.12$. These values correspond to an overall $S = 2$ spin ground state that fits with the absence of pronounced X-band EPR features. [**1**] and [**1**]$^-$ are thus the first isostructural imido metal complexes in two oxidation states in which both exhibit a high-spin state.

To shed further light on the electronic structures of [**1**]$^-$ and [**1**], DFT-(PBE, TPSSh, PBE0) and CASSCF/NEVPT2 calculations were performed.[36] All investigated computational methods afforded good to reasonable agreement with the XRD-, Mössbauer-, EPR- and SQUID data (bond lengths and angles, ΔE_Q, δ, g, A, D; Tables S3–S6†). According to the CASSCF calculations, in [**1**]$^-$, six electrons populate the two pairs of π/π*-interactions between the metal and imido ligand (Fig. 4, S43–S45†).

The two unpaired electrons in the antibonding combinations are thereby once metal centred (d_{xz}/π^*; Fe : N = 0.8 : 0.2; Löwdin population analysis) and once rather located at the

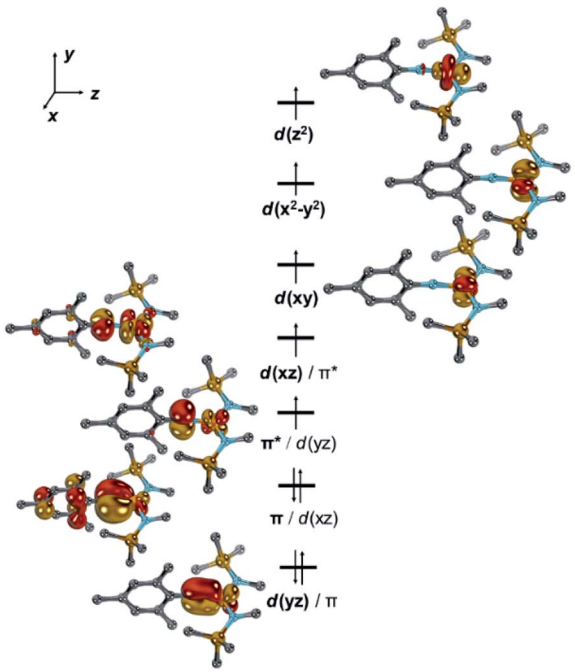

Fig. 4 Electronic structure of [**1**]$^-$ by CASSCF(11,9). Dipp groups were truncated by methyl groups, hydrogen atoms are omitted for clarity, one set of bonding and antibonding Dipp-centred π-orbitals is omitted for clarity.

ligand (π^*/d_{yz}; N : Fe = 0.6 : 0.4). This tentatively gives rise to the electronic structure of an imidyl iron(II) complex for $[\mathbf{1}]^-$. An oxidation state of iron(+II) is also substantiated by the Löwdin spin density of +0.66 a.u. at the imido nitrogen atom.

Neutral [**1**] features a quintet ground state ($\Delta E_{q/t}$ = +0.55 eV; $\Delta E_{q/sept}$ = +1.16 eV). The main configuration (c = 0.63) predicts thereby four unpaired electrons in d-orbitals (Fig. 5 and S40–S42†). Further two electrons are paired in the d_{xy} orbital, which combines with the imido ligand's p_x orbital (Fe : N = 7 : 3) and to a minor extent with the aromatic mesityl substituent. This gives overall rise to a formal d^6 (Fe^{II}) electron configuration of the metal and an electrophilic nitrene-type ligand. However, the second most important configuration (c = 0.21) relates to the π–π^* transition and thus suggests significant imidyl radical character.[5] This is further corroborated by accumulation of spin density at the imido nitrogen atom (−0.21 a.u.), which is suggestive of considerable antiferromagnetic character. Accordingly, the doubly excited resonance structure is also of relevance (c = 0.13), which overall leads to a population of the LUMO by formally 0.49 e^- and a shift of electron density to the ligand. Thus, when going from [**1**] to $[\mathbf{1}]^-$ the additional electron populates the antibonding π^* orbital, and weakens the metal–imido bond by formally −0.5. As such, the calculations highlight the electronic flexibility of the covalent iron–imido ligand interaction where the additional electron is not accepted by either the metal or the ligand, but by both. Since the electron is shared within the [FeNR] linkage, of course, rather similar Mössbauer spectroscopic features of [**1**] and $[\mathbf{1}]^-$ are expected, which aligns well with the experimental (*vide supra*) and calculated (Table S4†) parameters. It is thus reasonable to consider the imido iron unit in both complexes in its entirety, as proposed for a linear imido cobalt(II) compound.[37] Using the Enemark–Feltham notation for nitrosyl complexes[38] this leads to notations {FeNR}^{8} for [**1**] and {FeNR}^{9} for $[\mathbf{1}]^-$, and by that avoids singling out or overemphasizing a particular resonance structure.

Given these computed electronic structures of the "iron(II) imidyl" $[\mathbf{1}]^-$ as well as the "iron(II) nitrene" [**1**], we were curious if and how they would translate to differences in chemical reactivity. Both complexes showed only limited H-atom abstraction capabilities in case of 1,4-cyclohexadiene (after 24 h: [**1**]: 39%; $[\mathbf{1}]^-$: 73%). H atom abstraction from 1-hydroxy-2,2,6,6-tetramethyl-piperidine (TEMPO-H) was observed for [**1**] (24 h: 25% TEMPO by X-band EPR spectroscopy), whereas for $[\mathbf{1}]^-$ an ill-defined transformation of the imido complex was detected, without significant formation of TEMPO. These observations can be explained by the steric congestion. Possibly also to the ambivalent electronic nature of both complexes may contribute to the observed differences in reactivity. Reaction products of the H atom abstraction, *e.g.* the corresponding amides, could neither be identified nor isolated. This is attributed to subsequent reaction pathways such as scrambling of the amide ligands, as observed in a related cobalt system.[23] Subjecting [**1**] to an excess PEt_3 resulted in initial disappearance of the ^{31}P NMR signal of PEt_3. This phenomenon pointed to reversible coordination of the phosphine to the paramagnetic metal centre leading to spin polarisation and disappearance of the ^{31}P signal.[39] Addition of a stronger donor (2,2′-bipyridine) to such a reaction mixture after 24 h led immediately to reoccurrence of the PEt_3 signal, and more importantly small amounts of the nitrene transfer product $MesN{=}PEt_3$ (Scheme 2). This points to a slightly electrophilic behaviour of [**1**]. In contrast, $[\mathbf{1}]^-$ is completely inert towards PEt_3, as was also observed for the related cobalt complex.[23] On the other hand $[\mathbf{1}]^-$ reacts with CO to give MesNCO under nitrene transfer, whereas [**1**] does not.

Isonitriles (^{t}BuNC, MesNC) interact with both complexes, however no reaction product could be identified (*i.e.*, the

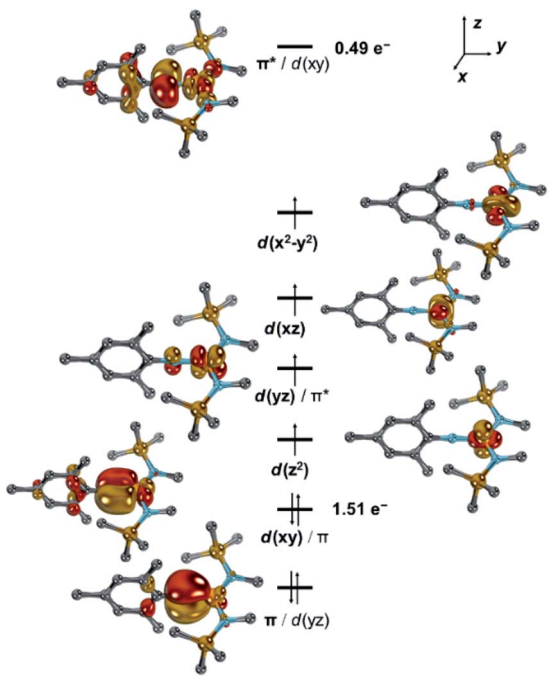

Fig. 5 Electronic structure of [**1**] by CASSCF(10,9). Dipp groups were truncated by methyl groups, hydrogen atoms are omitted for clarity, one set of bonding and antibonding Dipp-centred π-orbitals is omitted for clarity.

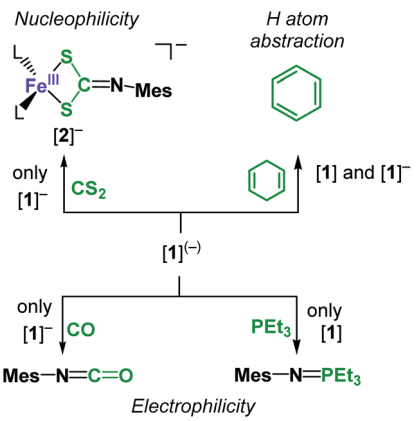

Scheme 2 Diverging reactivity of [**1**] and K{m}[**1**] towards nucleophiles, electrophiles, and C–H bonds.

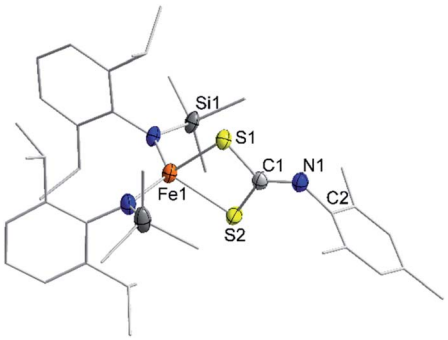

Fig. 6 Solid state structure of K{m}[**2**]. The K{m} cation as well as H atoms are omitted for clarity.

presumed carbodiimide RNC═NMes). Probing the nucleophilicity using CS_2 as a substrate revealed that [**1**] is unaffected for a prolonged period of time. $[\mathbf{1}]^-$ on the other hand reacted readily *via* insertion into the imido metal bond resulting in the dithiocarbonimidate complex $[L_2Fe(\eta^2\text{-}S_2C{=}NMes)]^-$, $[\mathbf{2}]^-$ (Fig. 6, Scheme 2). The assembly of a dithiocarbonimidate ligand *via* this reaction is remarkable, as in the coordination sphere of a metal it was only achieved by a [2 + 2] addition of organo isothiocyanates with transient terminal metal sulfides[40] or oxidation of isonitriles with metal persulfides.[41] The formation of $[\mathbf{2}]^-$ resembles the insertion of a carbodiimide into the iron(II) imide bond of the nucleophilic $[(Ph_2B(^tBuIM)_2)Fe(NDipp)]^-$. In both cases it likely results from an initial [2 + 2] cycloaddition of one of the C═X bonds with the M–N unit, in resemblance to the reaction of an imido nickel(II) complex with CO_2 or an imido iron(IV) complex with a carbodiimide (PhNCNPh).[26,42] $[\mathbf{2}]^-$ exhibits in solution a magnetic moment of 5.39 μ_B that is close to the spin-value of an $S = 5/2$ ion ($\mu_{s.o.} = 5.92\ \mu_B$). It shows that despite its mostly iron(II) imidyl character K{m}[**1**] reacts with an electrophile as an iron(III) imide, thus underscoring the electronic flexibility of the imido iron unit.

Conclusion

Concluding, we describe with $[Fe(NMes)L_2]^{0,-}$ (L = –N(Dipp)$SiMe_3$) a pair of isostructural imido iron complexes in two oxidation states. The electronic structures of the two compounds were comprehensively assessed, amongst others by EPR and ^{57}Fe Mössbauer spectroscopy and magnetometry, and revealed for both complexes a high-spin state. In line with the computational analysis and structural features, the neutral compound shares iron(II) nitrene and iron(III) imidyl character, whereas the reduced form is described best as an iron(II) imidyl. The change of the complexes' oxidation state is thus ligand and metal based, revealing the electronic flexibility of the imido metal bond. The ambiguity of the [FeNR] unit is reflected best by $[Fe(NMes)L_2]^-$ which shows a nucleophilic and electrophilic behaviour. Upon oxidation to $[Fe(NMes)L_2]^0$ the nucleophilicity is lost in accordance with a shift to a more nitrene-like electronic situation. We foresee these reactivity shifts to be relevant for directing NR group transfer reactivity of metal imidos towards different functionalities in organic substrates.

Data availability

All experimental procedures, spectral data, and computational data are included in the ESI.† Xyz coordinates may be obtained *via* the ESI,† output files can be obtained by D. M upon request. NMR/EPR/IR/Mössbauer raw data is so far only available upon request to C. G. W.

Author contributions

S. R. carried out the synthetic work and analytical characterization, including the crystallographic studies. S. D. recorded the SQUID and ^{57}Fe Mössbauer data, and both S. D. and F. M. analyzed the data. B. B., A. R., A. S. and C. L. recorded and analyzed the EPR data. C. S. performed the cyclic voltammetric analysis. D. M. performed the quantum chemical calculations. S. R. and C. G. W. wrote the manuscript with contributions from all authors.

Conflicts of interest

There are no conflicts to declare.

Acknowledgements

We thank the DFG for funding (grant 5627/4-1 for C. G. W., INST 186/1329-1 FUGG (SQUID magnetometer) for F. M.). D. M. thanks the RRZ Erlangen for computational resources. This project has received funding from the European Research Council (ERC) under the European Union's Horizon 2020 Research and Innovation Program (grant agreement no. 946184 for C. L. and no. 948185 for D. M.).

Notes and references

1 (*a*) P. Müller and C. Fruit, *Chem. Rev.*, 2003, **103**, 2905–2920; (*b*) L. Zhang and L. Deng, *Chin. Sci. Bull.*, 2012, **57**, 2352–2360; (*c*) Y. Park, Y. Kim and S. Chang, *Chem. Rev.*, 2017, **117**, 9247–9301; (*d*) Y. Liu, T. You, H.-X. Wang, Z. Tang, C.-Y. Zhou and C.-M. Che, *Chem. Soc. Rev.*, 2020, **49**, 5310–5358.

2 K. Kawakita, Y. Kakiuchi, H. Tsurugi, K. Mashima, B. F. Parker, J. Arnold and I. A. Tonks, *Coord. Chem. Rev.*, 2020, **407**, 213118.

3 (*a*) J. Strähle, *Angew. Chem.*, 1989, **101**, 957; (*b*) P. F. Kuijpers, J. I. van der Vlugt, S. Schneider and B. de Bruin, *Chem.–Eur. J.*, 2017, **23**, 13819–13829; (*c*) J. F. Berry, *Comments Inorg. Chem.*, 2009, **30**, 28–66.

4 K. Ray, F. Heims and F. F. Pfaff, *Eur. J. Inorg. Chem.*, 2013, **2013**, 3784–3807.

5 A. Grünwald, S. S. Anjana and D. Munz, *Eur. J. Inorg. Chem.*, 2021, **2021**, 4147–4166.

6 (*a*) R. A. Eikey and M. M. Abu-Omar, *Coord. Chem. Rev.*, 2003, **243**, 83–124; (*b*) N. Hazari and P. Mountford, *Acc. Chem. Res.*, 2005, **38**, 839–849; (*c*) J. L. Martinez, S. A. Lutz, H. Yang, J. Xie, J. Telser, B. M. Hoffman, V. Carta, M. Pink, Y. Losovyj and J. M. Smith, *Science*, 2020, **370**, 356–359.

7 E. R. King, E. T. Hennessy and T. A. Betley, *J. Am. Chem. Soc.*, 2011, **133**, 4917–4923.
8 M. J. T. Wilding, D. A. Iovan, A. T. Wrobel, J. T. Lukens, S. N. MacMillan, K. M. Lancaster and T. A. Betley, *J. Am. Chem. Soc.*, 2017, **139**, 14757–14766.
9 W. Mao, D. Fehn, F. W. Heinemann, A. Scheurer, D. Munz and K. Meyer, *Angew. Chem., Int. Ed.*, 2021, **60**, 16480–16486.
10 Y. Park, S. P. Semproni, H. Zhong and P. J. Chirik, *Angew. Chem., Int. Ed.*, 2021, **60**, 14376–14380.
11 Y. Dong, C. J. Lund, G. J. Porter, R. M. Clarke, S.-L. Zheng, T. R. Cundari and T. A. Betley, *J. Am. Chem. Soc.*, 2021, **143**, 817–829.
12 Y. Dong, J. T. Lukens, R. M. Clarke, S.-L. Zheng, K. M. Lancaster and T. A. Betley, *Chem. Sci.*, 2020, **123**, 4623.
13 K. M. Carsch, I. M. DiMucci, D. A. Iovan, A. Li, S.-L. Zheng, C. J. Titus, S. J. Lee, K. D. Irwin, D. Nordlund, K. M. Lancaster and T. A. Betley, *Science*, 2019, **365**, 1138–1143.
14 (*a*) A. G. Bakhoda, Q. Jiang, Y. M. Badiei, J. A. Bertke, T. R. Cundari and T. H. Warren, *Angew. Chem., Int. Ed.*, 2019, **58**, 3421–3425; (*b*) J. Moegling, A. Hoffmann, F. Thomas, N. Orth, P. Liebhäuser, U. Herber, R. Rampmaier, J. Stanek, G. Fink, I. Ivanović-Burmazović and S. Herres-Pawlis, *Angew. Chem., Int. Ed.*, 2018, **57**, 9154–9159; (*c*) M. J. B. Aguila, Y. M. Badiei and T. H. Warren, *J. Am. Chem. Soc.*, 2013, **135**, 9399–9406; (*d*) T. Corona, L. Ribas, M. Rovira, E. R. Farquhar, X. Ribas, K. Ray and A. Company, *Angew. Chem., Int. Ed.*, 2016, **55**, 14005–14008; (*e*) S.-L. Abram, I. Monte-Pérez, F. F. Pfaff, E. R. Farquhar and K. Ray, *Chem. Commun.*, 2014, **50**, 9852–9854.
15 F. Dielmann, D. M. Andrada, G. Frenking and G. Bertrand, *J. Am. Chem. Soc.*, 2014, **136**, 3800–3802.
16 C. M. Thomas, N. P. Mankad and J. C. Peters, *J. Am. Chem. Soc.*, 2006, **128**, 4956–4957.
17 S. D. Brown and J. C. Peters, *J. Am. Chem. Soc.*, 2005, **127**, 1913–1923.
18 I. Nieto, F. Ding, R. P. Bontchev, H. Wang and J. M. Smith, *J. Am. Chem. Soc.*, 2008, **130**, 2716–2717.
19 (*a*) L. Zhang, Y. Liu and L. Deng, *J. Am. Chem. Soc.*, 2014, **136**, 15525–15528; (*b*) Y. Liu, J. Du and L. Deng, *Inorg. Chem.*, 2017, **56**, 8278–8286.
20 Y. Gao, V. Carta, M. Pink and J. M. Smith, *J. Am. Chem. Soc.*, 2021, **143**, 5324–5329.
21 J. R. Winkler and H. B. Gray, in *Molecular Electronic Structures of Transition Metal Complexes I*, ed. D. M. P. Mingos, P. Day and J. P. Dahl, Springer Berlin Heidelberg, Berlin, Heidelberg, 2012, vol. 142, pp. 17–28.
22 D. A. Iovan and T. A. Betley, *J. Am. Chem. Soc.*, 2016, **138**, 1983–1993.
23 A. Reckziegel, M. Kour, B. Battistella, S. Mebs, K. Beuthert, R. Berger and C. G. Werncke, *Angew. Chem., Int. Ed.*, 2021, **60**, 15376–15380.
24 (*a*) A. Reckziegel, C. Pietzonka, F. Kraus and C. G. Werncke, *Angew. Chem., Int. Ed.*, 2020, **59**, 8527–8531; (*b*) R. Weller, L. Ruppach, A. Shlyaykher, F. Tambornino and C. G. Werncke, *Dalton Trans.*, 2021, **50**, 10947–10963.
25 (*a*) A. K. Verma, T. N. Nazif, C. Achim and S. C. Lee, *J. Am. Chem. Soc.*, 2000, **122**, 11013–11014; (*b*) S. D. Brown, T. A. Betley and J. C. Peters, *J. Am. Chem. Soc.*, 2003, **125**, 322–323; (*c*) S. C. Bart, E. Lobkovsky, E. Bill and P. J. Chirik, *J. Am. Chem. Soc.*, 2006, **128**, 5302–5303; (*d*) C. Ni, J. C. Fettinger, G. J. Long, M. Brynda and P. P. Power, *Chem. Commun.*, 2008, 6045; (*e*) J. J. Scepaniak, J. A. Young, R. P. Bontchev and J. M. Smith, *Angew. Chem., Int. Ed.*, 2009, **48**, 3158–3160; (*f*) R. E. Cowley, N. J. DeYonker, N. A. Eckert, T. R. Cundari, S. DeBeer, E. Bill, X. Ottenwaelder, C. Flaschenriem and P. L. Holland, *Inorg. Chem.*, 2010, **49**, 6172–6187; (*g*) H. Zhang, Z. Ouyang, Y. Liu, Q. Zhang, L. Wang and L. Deng, *Angew. Chem., Int. Ed.*, 2014, **53**, 8432–8436; (*h*) S. Kuppuswamy, T. M. Powers, B. M. Johnson, M. W. Bezpalko, C. K. Brozek, B. M. Foxman, L. A. Berben and C. M. Thomas, *Inorg. Chem.*, 2013, **52**, 4802–4811; (*i*) B. P. Jacobs, P. T. Wolczanski, Q. Jiang, T. R. Cundari and S. N. MacMillan, *J. Am. Chem. Soc.*, 2017, **139**, 12145–12148.
26 L. Wang, L. Hu, H. Zhang, H. Chen and L. Deng, *J. Am. Chem. Soc.*, 2015, **137**, 14196–14207.
27 M. J. T. Wilding, D. A. Iovan and T. A. Betley, *J. Am. Chem. Soc.*, 2017, **139**, 12043–12049.
28 A. Sridharan, A. C. Brown and D. L. M. Suess, *Angew. Chem., Int. Ed.*, 2021, **60**, 12802–12806.
29 C. Schneider, S. Demeshko, F. Meyer and C. G. Werncke, *Chem.–Eur. J.*, 2021, **27**, 6348–6353.
30 Y. Sanakis, P. P. Power, A. Stubna and E. Münck, *Inorg. Chem.*, 2002, **41**, 2690–2696.
31 A. Eichhöfer, Y. Lan, V. Mereacre, T. Bodenstein and F. Weigend, *Inorg. Chem.*, 2014, **53**, 1962–1974.
32 E. C. Alyea, D. C. Bradley, R. G. Copperthwaite, K. D. Sales, B. W. Fitzsimmons and C. E. Johnson, *J. Chem. Soc. D*, 1970, 1715–1716.
33 K. E. Aldrich, B. S. Fales, A. K. Singh, R. J. Staples, B. G. Levine, J. McCracken, M. R. Smith and A. L. Odom, *Inorg. Chem.*, 2019, **58**, 11699–11715.
34 P. Gütlich, *Mössbauer Spectroscopy and Transition Metal Chemistry. Fundamentals and Applications*, Springer Berlin/Heidelberg, Berlin, Heidelberg, 2011.
35 (*a*) M. R. Anneser, G. R. Elpitiya, J. Townsend, E. J. Johnson, X. B. Powers, J. F. DeJesus, K. D. Vogiatzis and D. M. Jenkins, *Angew. Chem., Int. Ed.*, 2019, **58**, 8115–8118; (*b*) K. Searles, S. Fortier, M. M. Khusniyarov, P. J. Carroll, J. Sutter, K. Meyer, D. J. Mindiola and K. G. Caulton, *Angew. Chem., Int. Ed.*, 2014, **53**, 14139–14143.
36 F. Neese, F. Wennmohs, U. Becker and C. Riplinger, *J. Chem. Phys.*, 2020, **152**, 224108.
37 X.-N. Yao, J.-Z. Du, Y.-Q. Zhang, X.-B. Leng, M.-W. Yang, S.-D. Jiang, Z.-X. Wang, Z.-W. Ouyang, L. Deng, B.-W. Wang and S. Gao, *J. Am. Chem. Soc.*, 2017, **139**, 373–380.
38 J. H. Enemark and R. D. Feltham, *Coord. Chem. Rev.*, 1974, **13**, 339–406.
39 R. Weller, A. Gonzalez, H. Gottschling, C. Hänisch and C. G. Werncke, *Z. Anorg. Allg. Chem.*, 2022, e202100338.
40 (*a*) J. Ahmed, K. Itoh, I. Matsuda, F. Ueda, Y. Ishii and J. A. Ibers, *Inorg. Chem.*, 1977, **16**, 620–624; (*b*) K.-E. Lee,

X. Chang, Y.-J. Kim, H. S. Huh and S. W. Lee, *Organometallics*, 2008, **27**, 5566–5570; (*c*) Y.-J. Kim, H.-T. Jeon, K.-E. Lee and S. W. Lee, *J. Organomet. Chem.*, 2010, **695**, 2258–2263; (*d*) R. O. Harris, J. Powell, A. Walker and P. V. Yaneff, *J. Organomet. Chem.*, 1977, **141**, 217–229.

41 R. D. Adams, B. Captain, O.-S. Kwon and S. Miao, *Inorg. Chem.*, 2003, **42**, 3356–3365.

42 D. J. Mindiola, R. Waterman, V. M. Iluc, T. R. Cundari and G. L. Hillhouse, *Inorg. Chem.*, 2014, **53**, 13227–13238.